Triton angular distributions from the ^{7}Li$(\gamma,t)\alpha$ reaction near threshold

V. P. Likhachev, M. N. Martins, M. T. F. da Cruz, and J. D. T. Arruda-Neto
Laboratório do Acelerador Linear, Instituto de Física da Universidade de São Paulo, Caixa Postal 66318, 05315-970, São Paulo, SP, Brazil

L. P. Geraldo and R. Semmler
Instituto de Pesquisas Energéticas e Nucleares-IPEN/CNEN-SP, São Paulo, SP, Brazil

J. F. Dias
Instituto de Física da Universidade Federal do Rio Grande do Sul, Porto Alegre, RS, Brazil

(Received 26 August 1998)

Angular distributions of tritons emitted in the reaction ^{7}Li$(\gamma,t)\alpha$ have been measured for two photon energy intervals (6.4–6.7 and 8.5–9.0 MeV), and θ_t between 30° and 150°. Monochromatic photons from neutron capture reactions of the IPEN/CNEN-SP IEA-R1 research reactor were used. The measured data were analyzed in the framework of an α-cluster model for the ^{7}Li structure. Results are in good agreement with a recent measurement of the azimuthal cross section asymmetry.
[S0556-2813(99)04601-4]

PACS number(s): 25.20.Lj, 25.10.+s

The ground state of ^{7}Li$(J^\pi=3/2^-)$ is a typical clustered nuclear system, consisting mostly of an α-particle and a triton [1], with other components of the wave function playing secondary roles [2]. The study of cluster properties in nuclei gained a new impetus due to microscopic calculations based on the method of resonating group (MRG) [3,4] and also of multicluster models [5–8]. Those calculations adequately describe the main static characteristics of nuclear systems and achieved remarkable progress in the description of the radiative capture of clusters (like $t+\alpha \rightarrow {}^7\mathrm{Li}+\gamma$ [9]).

According to these models the $E1$ multipole dominates the differential cross section of the ^{7}Li$(\gamma,t)\alpha$ reaction at low photon energies. $E1$ transitions give rise to the S and D waves of the final state continuum:

$$\left(\frac{3^-}{2}\right) \xrightarrow{E1} S_{(1/2^+)} + D_{(3/2^+,5/2^+)},$$

where the values in parentheses indicate total angular momentum and parity, and the D wave is split by the spin-orbit interaction into $3/2^+$ and $5/2^+$ states. Near the threshold the process is dominated by the S wave, due to the additional centrifugal barrier for the D wave, which is important in this region. At higher energies, according to MRG [9] and cluster model calculations [10], the D wave is dominant. There is a region where the contributions of the S and D waves are comparable. This transition from the dominance of the S to the D wave leads to changes in the angular distributions of the final particles in the case of excitation by unpolarized photons, or to oscillations in the Σ-asymmetry for polarized photons [10].

The aim of the present work is the accurate measurement of angular distributions of tritons emitted in the ^{7}Li$(\gamma,t)\alpha$ reaction, at two characteristic energy bins: 6.4–6.7 MeV, where the S and D waves contributions are comparable, and 8.5–9 MeV, where the contribution of the D wave is dominant, in order to: (i) clarify the experimental situation of triton angular distributions at low energies, using monochromatic photons with energies below the thresholds of contaminating reactions, and (ii) to test the prediction of the potential cluster model with attractive local potential and forbidden states [11].

The experiment has been carried out at the IPEN/CNEN-SP IEA-R1 research reactor, using monochromatic photon beams from neutron capture reactions [12]. The neutron targets were located at the midpoint of the BH4-12 tangential beam hole of the reactor (Fig. 1). The system allows (using different neutron target materials) the use of up to 30 discrete photon lines with energies from 5 to 11 MeV and energy resolution of a few eV.

The thermal neutron flux at the target position was $\sim 6.2 \times 10^{11}$ n/cm^2 s, monitored by a self-powered neutron detector (SPND) installed close to the neutron target. The photon flux is collimated by a long ($\sim$228 cm) lead collimator. In order to reduce neutron contamination, the beam is filtered after collimation by 36.5 cm of polyethylene and 9.5 cm of borated paraffin. The target consists of a 45×70 mm^2, self-supporting metallic natural lithium foil (92.5% ^{7}Li and 7.5% ^{6}Li), 100 μm or 50 μm thick (depending on the photon

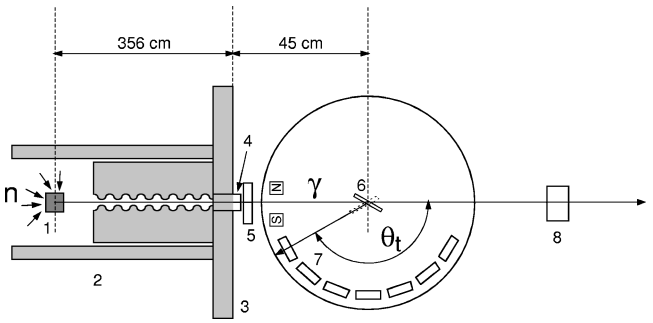

FIG. 1. Experimental setup: (1) neutron target; (2) lead collimator; (3) concrete wall; (4) polyethylene; (5) borated paraffin; (6) Li target; (7) Si detectors; (8) Ge(Li) detector.

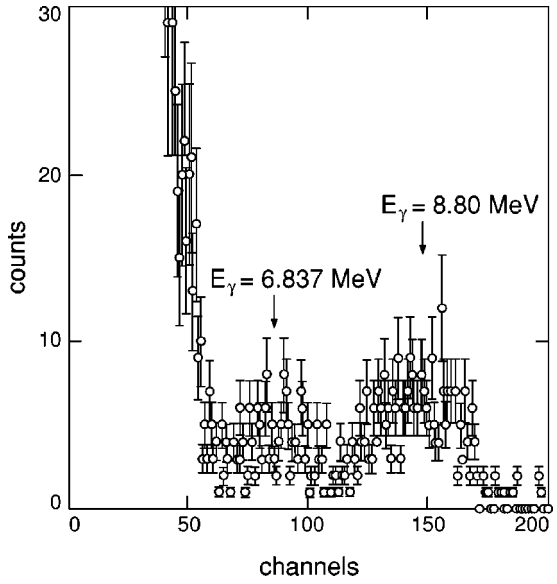

FIG. 2. Typical triton spectrum obtained at $E_\gamma \sim 8.80$ MeV.

energy). The target was placed inside a vacuum chamber, which also housed the silicon strip detectors and a calibrated alpha source for energy calibration. The beam spot on the target was 3×6 cm^2, for a target tilt of 30°.

The charged products of the reaction were detected by an arrangement of seven silicon strip detectors [13], located at triton emission angles, θ_t, equal to 30°, 50°, 70°, 90°, 110°, 130° and 150°. The distance from the detector to the center of the target was 17 cm, with full detector (all 16 strips) solid angle, $\Delta\Omega$, of 0.09 sr. The detector angular acceptance (for a point target) was $\Delta\theta_p = \pm 8.4°$ and $\Delta\phi = \pm 8.4°$. The actual beam dimensions increased the detector angular acceptance to $\Delta\theta_p = \pm 12°$ and $\Delta\phi = \pm 11°$, according to a Monte Carlo simulation [14].

Two neutron targets were used in the experiment, Ti and Ni. The Ti target photon spectrum presents two strong lines: 6.418 and 6.759 MeV [15] (weighted average 6.56 MeV), which sum 80% of the intensity responsible for the emission of tritons with energies above the detection threshold. The rest of the intensity (20%) is distributed among several low intensity lines. For the Ni target, the photon spectrum presents two strong lines at 8.998 and 8.533 MeV [15] (weighted average 8.80 MeV), which concentrate 60% of the total intensity and a line at 6.837 MeV with 15% of the total intensity. The rest of the intensity (25%) is distributed among several low intensity lines.

Within the conditions of our experiment ($E_\gamma < 10$ MeV) only the reactions

$$\gamma + {}^7\mathrm{Li} \rightarrow t + \alpha \qquad (1)$$

and

$$n + {}^6\mathrm{Li} \rightarrow t + \alpha \qquad (2)$$

may contribute to the measured spectra. The second one is caused by neutrons from both beam contamination and background in the experimental area, which interact with the ^{6}Li present in the target. Other reactions either have thresholds above the photon energies used, or negligible cross sections.

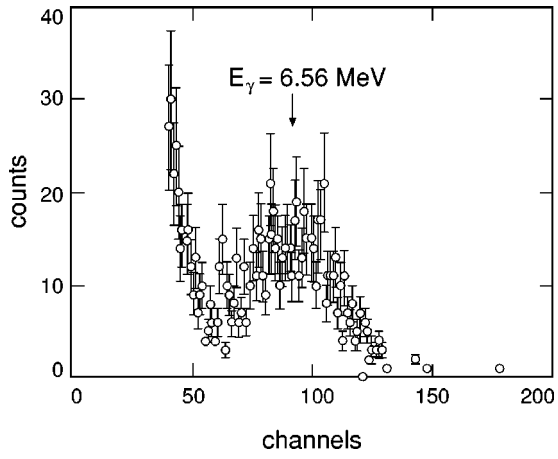

FIG. 3. Typical triton spectrum obtained at $E_\gamma \sim 6.56$ MeV.

Both reactions produce the same particles in the final states, but with different energy spectra. Due to the reaction kinematics, α-particles carry less energy than tritons. Moreover, the energy loss in the target is larger for alphas than for tritons. For those reasons, the number of α particles detected is much smaller than that of tritons, and their counts are concentrated in the low-energy part of the spectrum.

The background from reaction (2) was evaluated using a dummy neutron target (with very low intensity photons). The dominant contribution comes from thermal neutrons in the experimental area, the neutron contamination in the beam being very small. The thermal neutron background was reduced with a Cd shield around the scattering chamber.

Figure 2 shows a typical spectrum, measured using the Ni neutron target and a 150 μm thick Li target. One can clearly see the background at the lower channels and two bumps. The high energy bump, peaked around channel 150 ($\sim$3.5 MeV), corresponds to tritons produced by reaction (1), induced by photons from the 8.80 MeV lines; the other one, peaked around channel 90 ($\sim$2.3 MeV), corresponds to tritons produced both by reactions (2) and (1), the last induced by the secondary photon line at 6.837 MeV.

Figure 3 shows an analogous spectrum obtained using the Ti neutron target and a 50 μm thick Li target. This spectrum presents a single bump, formed by tritons produced by reaction (1), induced by the principal photon line (6.56 MeV) with a small contribution ($\sim$5%) from reaction (2). This contribution was taken into account in the analysis.

The differential cross sections obtained experimentally in this work were normalized to unity at $\theta = 90°$, and are shown in Figs. 4 and 5 by the open circles. Those figures also show results from measurements using real [16] (band 1) and virtual [17] (band 2) photons. The bands were obtained by reconstructing the differential cross sections from the published Legendre coefficients. The absolute values of the cross sections presented in Refs. [16] and [17] are $\sim$20% different. Both results were normalized to unity at 90°, in order to allow a better visualization. The dashed curve represents the results obtained in the framework of the binary cluster potential model [10], also normalized to unity at 90°. According to this model, the $E1$ component of the differential cross section is dominated around 9 MeV by the D scattering wave, resulting in an angular dependence with a maximum at 90°. The behavior is in good agreement with our measure-

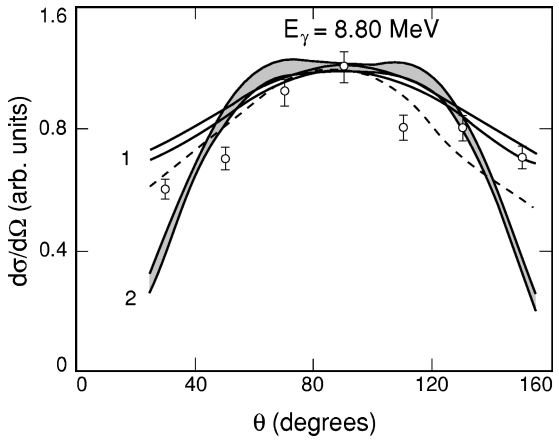

FIG. 4. Differential cross section for $E_\gamma \sim 8.80$ MeV. This work (data points); measurements with real photons from Ref. [16] (band 1); measurements with virtual photons from Ref. [17] (band 2); binary cluster potential model calculation from Ref. [10] (dashed curve). All results are normalized to unity at 90°.

ment and that of Ref. [16], and not with Ref. [17]. According to this model [11], the contributions from *S* and *D* scattering waves are comparable around 6.5 MeV, resulting in an isotropic angular distribution. Again, there is good agreement between our results and those from Ref. [16].

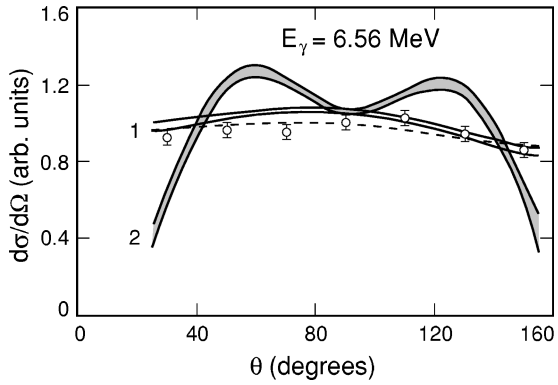

FIG. 5. Differential cross section for $E_\gamma \sim 6.56$ MeV (see caption of Fig. 4).

The agreement between measurements and the predictions of the binary cluster potential model indicates that the characteristic change in the angular distributions of the emitted tritons, which is a signature of the overflow of *S* and *D* scattering waves of $E1$ transitions, is correctly described by the model. This conclusion is corroborated by the results of a Σ-asymmetry measurement for the reaction $^7\mathrm{Li}(\vec{\gamma},t)\alpha$ performed in this energy region [10].

[1] K. Windermuch and J. Tan, *Unified Nuclear Theory* (Vieweg, Braunschweig, 1977).

[2] S. B. Dubovichenko and M. A. Zhusupov, Sov. J. Nucl. Phys. **39**, 1378 (1984).

[3] M. Unkelbach and H. M. Hofmann, Phys. Lett. B **261**, 211 (1991).

[4] M. Unkelbach and H. M. Hofmann, Few-Body Syst. **11**, 143 (1991).

[5] V. I. Kukulin, V. T. Voronchev, T. D. Kaipov, and R. A. Eramzhyan, Nucl. Phys. **A517**, 221 (1990).

[6] B. V. Danilin, M. V. Zhukov, S. N. Ershov, F. A. Gareev, R. S. Kurmanov, J. S. Vaagen, and J. M. Bang, Phys. Rev. C **43**, 2835 (1991).

[7] G. G. Ryzhikh, R. A. Eramzhyan, V. I. Kukulin, and Yu. M. Tchuvil'sky, Nucl. Phys. **A563**, 247 (1993).

[8] A. Eskandarian, D. R. Lehman, and W. C. Parke, Phys. Rev. C **38**, 2341 (1988).

[9] T. Kajino, Nucl. Phys. **A460**, 559 (1986); T. Kajino, G. F. Bertsch, and Ken-ichi Kubo, Phys. Rev. C **37**, 512 (1988).

[10] N. A. Burkova, V. V. Denyak, R. A. Eramzhyan, I. G. Evseev, V. M. Khvastunov, V. P. Likhachev, S. A. Paschuk, and M. A. Zhusupov, Nucl. Phys. **A586**, 293 (1995); N. A. Burkova, M. A. Zhusupov, and R. A. Eramzhyan, Report No. P-0551, Inst. Nucl. Research, Acad. of Sci., USSR, 1987.

[11] V. G. Neudatchin, V. I. Kukulin, V. L. Korotkikh, and V. P. Korennoy, Phys. Lett. **34B**, 581 (1971); V. I. Kukulin, V. G. Neudatchin, and Yu. F. Smirnov, Nucl. Phys. **A245**, 429 (1975).

[12] R. Semmler and L. P. Geraldo, Nucl. Instrum. Methods Phys. Res. A **336**, 171 (1993).

[13] V. P. Likhachev, J. F. Dias, M. I. Yoneama, M. N. Martins, J. D. T. Arruda-Neto, C. C. Bueno, V. Perevertailo, and O. Frolov, Nucl. Instrum. Methods Phys. Res. A **376**, 455 (1996).

[14] V. P. Likhachev, M. N. Martins, J. D. T. Arruda-Neto, C. C. Bueno, M. Damy de S. Santos, I. G. Evseev, J. A. L. Gonçalves, O. A. M. Helene, S. A. Paschuk, and H. R. Schelin, Nucl. Instrum. Methods Phys. Res. A **390**, 251 (1997).

[15] M. A. Lone, R. A. Leavitt, and D. A. Harrison, At. Data Nucl. Data Tables **26**, 512 (1981).

[16] G. Junghans, K. Bangert, U. E. P. Berg, R. Stock, and K. Wienhard, Z. Phys. A **291**, 353 (1979).

[17] D. M. Skopik, J. Asai, E. L. Tomusiak, and J. J. Murphy, II, Phys. Rev. C **20**, 2025 (1979).